Nuclear liquid-drop model and surface-curvature effects

K. Pomorski[1,2] and J. Dudek[1]

[1]*Institut de Recherches Subatomiques, IN_2P_3-CNRS/Université Louis Pasteur F-67037 Strasbourg Cedex 2, France*

[2]*Katedra Fizyki Teoretycznej, Uniwersytet Marii Curie-Skłodowskiej, PL-20031 Lublin, Poland*

(Received 7 May 2002; revised manuscript received 23 January 2003; published 29 April 2003)

Nuclear liquid-drop model is revisited and an explicit introduction of the surface-curvature terms is presented. The corresponding parameters of the extended classical energy formula are adjusted to the contemporarily known nuclear binding energies and fission-barrier heights. Using 2766 binding energies of nuclei with $Z \geqslant 8$ and $N \geqslant 8$ it is shown that the performance of the new approach is improved by a factor of about 6, compared to the previously published liquid-drop model results, in terms of the masses (new rms deviation $\langle \delta M \rangle = 0.698$ MeV) and the fission barriers by a factor of about 3.5 (new rms deviation of the fission barriers of isotopes with $Z > 70$ is $\langle \delta V_B \rangle = 0.88$ MeV). The role of the nuclear surface-curvature terms and their effects on the description of the experimental quantities are discussed in detail. For comparison, the parameters of the more ''traditional'' classical energy expressions are refitted, taking into account the nuclear masses known today and the performances of several variants of the model are compared. The isospin dependence in the new description of the barriers is in a good agreement with the extended Thomas-Fermi approach. It also demonstrates a good qualitative agreement with the fission lifetime systematics tested on the long chain of Fermium isotopes known experimentally. The new approach offers a very high stability in terms of the extrapolation from the narrower range of nuclides to a more extended one—a property of particular interest for the contemporary exotic beam projects: the corresponding properties are illustrated and discussed. The new description of the fission barriers being significantly improved, in particular, the new calculated barriers being lower, flatter, but stiffer against high-multipolarity deformations. The chances for ''extra'' stabilization of the hyperdeformed minima at high spin increase, thus calling for the new total energy Strutinsky-type calculations.

DOI: 10.1103/PhysRevC.67.044316 PACS number(s): 24.75.+i, 25.85.−w, 25.60.Pj, 25.70.−z

I. INTRODUCTION

It is more than 60 years now since the first successful application of the charged liquid-drop model to describe the nuclear binding energies [1,2]. Brilliant extensions of the Bethe-Weizsäcker nuclear drop concept by Meitner and Frisch [3] and by Bohr and Wheeler [4] have been obtained in 1939 and used to explain the nuclear fission phenomenon. Since then many papers have been devoted to the nuclear liquid-drop model formalism and its improvements. Various new terms in the corresponding energy expressions have been proposed but the basic concept of the charged liquid drop which could deform and fission remained valid. It is worth reminding at this point that already in 1953 Hill and Wheeler concluded on the basis of the Fermi gas model, Ref. [5], that a curvature dependent term proportional to $A^{1/3}$ should exist in the liquid-drop energy functional. The curvature term was later studied in Ref. [6], where its magnitude was adjusted to the experimental fission-barrier heights known at that time.

Deformation-dependent classical energy expressions can be seen as functions of two groups of variables that describe, respectively, the nucleus itself (Z,N) and its shape represented by an ensemble of the deformation parameters, here denoted $\{\alpha\}$. Typically, the surface energy is written as a product $E_s(Z,N;\{\alpha\}) = f(Z,N)g(\{\alpha\})$, where the first factor is usually parametrized by introducing a few adjustable constants e.g., $f(N,Z) = p_0 + p_1[(N-Z)/(N+Z)]^2$ or any other expression of this type that is found performant. p_1 and p_2 are adjustable constants, whose number does not need to be limited to 2. As it has been discussed already by other authors, in a more careful approach the nuclear surface energy can be seen as contributed by *two* different but related geometrical elements: the numerical value of the surface area and the surface's average curvature. Such a formulation implies a different form of the surface energy expression, $E_s(Z,N;\{\alpha\}) = f_a(Z,N)g_a(\{\alpha\}) + f_c(Z,N)g_c(\{\alpha\})$, where indices a and c refer to area and curvature, respectively, and where the deformation dependencies in g_a and g_c are different. Moreover, in the spirit of the classical nuclear energy models, the corresponding factors $f_a(Z,N)$ and $f_c(Z,N)$ are to be adjusted separately. By refitting all the adjustable parameters of the classical energy expression to the experimental masses of over two thousand nuclei as well as on the fission barriers we are going to look for the most performant parametrization to be used in conjunction with the Strutinsky-type formalism. In such an approach, all the terms including the surface energy term will be represented as optimally as possible in a global fit. One may expect that the surface area contribution $\sim f_a g_a$ should be a dominating factor since the traditional liquid-drop model without explicit use of the curvature-energy term performed quite well already. The surface-curvature term is expected to be smaller and play a role of correction. We will demonstrate that such a fit is possible and corresponds to a significant improvement of performance of the liquid-drop model formula. In particular, the new rms deviation will be shown to be $\langle \delta M \rangle = 0.698$ MeV compared to $\langle \delta M \rangle = 0.732$ MeV within the traditional approach, and the new fission-barrier rms

deviation[1] for nuclei with $Z>70$, $\langle \delta V_B \rangle = 0.88$ MeV, compared to $\langle \delta V_B \rangle = 5.58$ MeV.

Several studies performed in the past, of the contributions coming from the surface curvature to the total energy, aimed at estimating its value using a more elementary (microscopic) concepts of the nuclear interactions, both for the finite nuclei and for the semi-infinite nuclear matter media. Some of the corresponding papers are mentioned below; much more details about that evolution can be found in the articles quoted therein. In particular, using the energy-density formalism of Ref. [7] combined with the macroscopic formulation of the curvature-energy expressions of Myers and Świątecki, [8], Stocker, Ref. [9], pointed to the compatibility of the curvature-energy estimates coming from the two approaches. Grammaticos, Ref. [10], using the Skyrme-type functional, but limiting himself to the terms of the order of $\hbar^2$, was able to obtain what could be considered as a reasonable estimate for the curvature energy; stressing however that the results are sensitive to the details of the energy functional and pointing to the necessity of including higher-order terms. This has been done for instance in Ref. [11], where also a comparison of the results of various calculations and estimates known at the time of publication can be found. However, the main results obtained by the authors, were compatible with the earlier theoretical predictions. A more distinct link between microscopic and macroscopic models was proposed in Ref. [12], where various terms of the droplet model were derived from the Skyrme interaction, in the framework of the extended Thomas-Fermi (ETF) model. The problem of self-consistency, when approaching the issue of the curvature energy, has been addressed in Ref. [13]; no major influence of this aspect of the formalism on the final result has been found. Relativistic mean-field theory within semiclassical approach has been applied, Ref. [14], to the semi-infinite nuclear matter concluding that the relativistic and the more traditional methods give in essence compatible results. Extension to the relativistic but quantum approaches has been studied in Ref. [15], with the conclusion that also within the relativistic approaches the semiclassical and fully quantum approaches give consistent, comparable results. Similar physical goals but within relativistic Hartree approximation have been approached in Ref. [16], and sensitivity of the final result to the related physical quantities such as the (in)compressibility coefficient and nucleonic effective-mass has been discussed. A detailed, recent analysis of the problem of the surface and curvature energies using Skyrme-type interactions, but aiming principally at the astrophysical applications can be found in Ref. [17], see also references therein.

Let us stress that the above mentioned developments addressed first of all the problem of an existence of relationships between the nuclear curvature energy and a microscopic representation of the nuclear forces; together with the role of such elements and mechanisms as the order of expansion in the extended Thomas-Fermi model, type of the Skyrme forces, comparison between the semiclassical and the quantum calculation results, as well as the possible influence of the relativistic effects. All these studies point coherently to the result that the first-order curvature coefficient should be of the order of, typically, 5 to 15 MeV. At the same time, many phenomenological approaches based directly on the *global fits* to the experimental data pointed to the value very close to zero. In fact, in several studies the corresponding term was often altogether neglected and the discrepancy mentioned turned into a kind of a ''curvature anomaly'' problem.[2]

There is also another group of studies that were focused more specifically on the calculations of the nuclear masses and/or the deformation dependence in the classical energy expressions that supplemented with the Strutinsky and pairing quantum energy terms, could be used for studying such problems as nuclear fission, super and hyperdeformations and more generally the shape coexistence phenomena. A few years ago, a realistic Thomas-Fermi (TF) model has been developed by Myers and Świątecki [18], which describes masses of known nuclei with high accuracy. The corresponding rms deviation between the experimental [19] and theoretical binding energies for 1654 isotopes amounts to 0.655 MeV only. In the last decade, more than one thousand masses of new isotopes have been measured and in the new edition of the Strasbourg Chart of Nuclides [20], one can find 2766 binding energies of the isotopes with the proton and neutron numbers larger that $Z=N=8$ (cf. Fig. 1). The rms deviation of the TF estimates for these 2766 masses is 0.758 MeV and shows a high numerical precision of the model as well as a good accuracy of the shell and pairing energies obtained in Ref. [21] that the TF model adopts. Fission-barrier heights evaluated on the basis of the Thomas-Fermi model [18,22] are also in a rather good agreement with the experimental data.

A significant progress in the self-consistent methods has taken place in the recent years as well. For instance, the Hartree-Fock mass formula of Tondeur *et al.*, Ref. [23], that employs the effective $MSk7$ Skyrme interaction was able to reproduce the 1888 experimental binding energies with the rms deviation of 0.738 MeV. This rms deviation increases to

[1]Throughout the paper, we use the following definition of the rms deviation, $\chi = \sqrt{1/(n-1)\Sigma_{j=1}^{n}(f_j - f_j^{expt.})^2}$, where $f_j^{expt.}$ denotes the experimental value at the data point j and f_j is the corresponding calculated value.

[2]The curvature-energy contribution is not the only term proportional to $A^{1/3}$, the nuclear matter compression mechanism leads to the same A—but a different deformation dependence. We have verified by two independent fits (the one that contains the first-order curvature effects but ignores the compression energy contribution and another one that takes simultaneously into account both of these terms) that the final results for the mass and fission-barrier fits are very similar in both cases. More precisely, in the latter case the curvature coefficient turns out to be nearly twice as large as in the former, but its increase is compensated by an opposite sign contribution from the compression. We conclude that the model does not provide enough sensitivity at present to distinguish between these two mechanisms. In the present analysis, the compression effects are not taken explicitly into account.

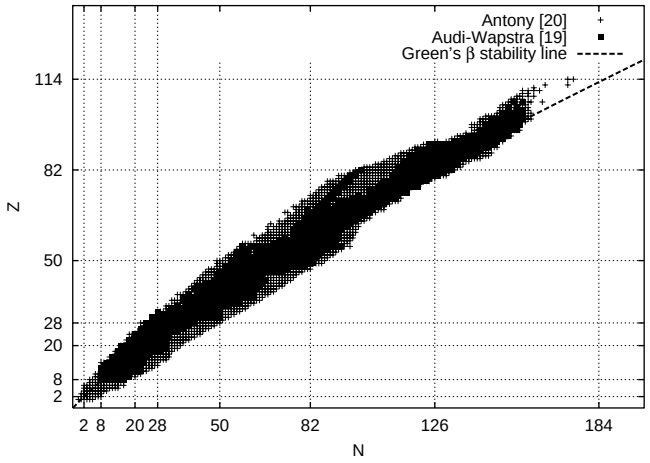

FIG. 1. The chart of isotopes for which the experimental binding energies are known. The crosses correspond to data from the compilation of Antony [20], while black squares to the data from Ref. [19] on which the analysis of Myers and Świątecki [18] has been based.

only 0.828 MeV when one makes the comparison with 2766 experimental masses taken from the table [20].

At present, the self-consistent and the macroscopic-microscopic methods play both their important roles in the nuclear structure calculations. While the latter are very well suited, for, e.g., the ''automatic'' large scale calculations of the total nuclear energy surfaces, fission barriers, high spin properties, shape-isomerism studies, and/or numerous excited particle-hole configurations; the former are extremely useful in the detailed theoretical description of the nuclear states whose global features are already known. The simplicity of the macroscopic nuclear drop formalism together with the clear physical meaning of its parameters add definitely to its attractiveness. It is easy to apply and thus frequently used, in particular, in estimating the fusion and fission cross sections in heavy ions reactions.

A particular motivation for the present work is to obtain a new set of parameters of the liquid-drop model adjusted to the up-to-date experimental masses and fission barriers, while taking a particular care of the surface-curvature aspects of the model. This is of special importance when studying the exotic nuclear shapes, such as the nuclear hyperdeformation and/or the nuclear path to fission (e.g., the bimodal or more complex fission phenomena).

A starting point of our analysis is the well known traditional liquid-drop nuclear mass expression of Myers and Świątecki (MS-LD) [24]. This expression was quite successful in reproducing the nuclear masses, but it is known that in the light nuclei it overestimates the fission-barrier heights by up to about 10 MeV [25]. The MS-LD barriers are also higher than those evaluated by Sierk [26] within the Yukawa-folded-interaction macroscopic model.

It is obviously important to assure the stability of the final result with respect to the cutoff in terms of the number of multipoles used. All the fission-barrier heights presented in this paper were obtained by minimizing with respect to the deformation parameters β_λ of even λ up to $\lambda_{max}=14$. In order to test the stability of our minimization procedure with respect to this cutoff, we have performed additional test minimizations using the Trentalange-Koonin-Sierk (TKS) family of shapes defined in Ref. [27]. The multipole and the TKS parametrizations clearly differ, yet the resulting fission barriers almost coincide when number of the β_λ parameters is sufficiently large. Going beyond $\lambda_{max}=14$ does not change the final fission-barrier results in the studied cases by more than a couple of 100 keV for the highest barriers calculated here, i.e., in the $A\sim 80$ mass range, while for the heavier nuclei the modifications are of the order of 12 keV, an accuracy totally sufficient in the present context.

It turns out that, to obtain a given accuracy one needs typically twice as many multipoles as TKS deformation parameters. However, we found out that the β_λ parametrization is easier to handle than the TKS one, when performing the numerical minimization of the potential energy surfaces. More precisely, in constructing automatic algorithms of minimization over the nuclear shapes, it is important to assure its stable behavior when moving in the deformation space. As it happens, various parametrizations lead to different behavior in this respect. In particular, when approaching the limits of applicability of the shape parametrization (e.g., the deformation-parameter values for which the distance from the origin of the reference frame to the points on the surface approaches zero) also some derivatives involving deformation parameters have a tendency to vary rapidly, thus destabilizing the minimization algorithm. Direct calculations show that the traditional multipole parametrization offers more stable behavior as compared to the one by Trentalange-Koonin-Sierk of Ref. [27] and thus faster algorithms. This becomes important in the detailed Strutinsky calculations, where 20–30 deformation degrees of freedom are treated at the same time.[3] Needless to say, no result of this paper depends on any of those ''technical'' details.

Direct calculations show that the Yukawa-folded-interaction model, which gives rather reasonable estimates of the fission barriers, is too soft in directions orthogonal to the fission path especially at the large nuclear elongation. It will be of great interest, trying to combine (and we will demonstrate that it is possible) an improved description of the fission barriers together with a better description of the above mentioned stiffness behavior within one single approach.

The paper is organized as follows. The actual version of the liquid-drop model used is described in Sec. II. In Sec. III we specify the way in which the parameters were determined, and we present the best sets of parameters for various variants of the LD models.

Our results concerning the fission barriers are presented in Sec. IV. The paper is summarized in Sec. V.

II. LIQUID-DROP MODEL AND MICROSCOPIC ENERGY FUNCTIONAL

We are going to recapitulate briefly the main ideas of the leptodermous expansion [28] of the energy-density func-

[3]Modern versions of the Strutinsky method depart more and more from the deformation-mesh technique by using the explicit deformation-minimization technique in which case their functioning becomes more similar to the constrained Hartree-Fock methods.

tional, in order to introduce the presentation of the role of the nuclear surface-curvature terms. Within this model the nuclear part of the total energy of a nucleus can thus be given by the well known expression

$$E = b_{\rm vol} A + b_{\rm surf} A^{2/3} + b_{\rm cur} A^{1/3} + b_{\rm curG} A^0 + \cdots, \quad (1)$$

the Coulomb part will be introduced later.

It is instructive to study the properties of expression (1) in the case of spherical nuclei for which the leptodermous espansion of the energy functional can be written as follows:

$$E = b_{\rm vol} A + \int_V (\eta - b_{\rm vol}\rho) d^3\mathbf{r} \quad (2a)$$

$$= b_{\rm vol} A + \int_\Sigma R^2\, d\Omega \int_0^\infty (\eta - b_{\rm vol}\rho) \frac{r^2}{R^2} dr, \quad (2b)$$

where R (usually represented as $R = r_0 A^{1/3}$) is the radius of the spherical surface, ρ is the one-body density of the nuclear matter in nucleus, and η is the energy density.

Making use of the identity,

$$\frac{r^2}{R^2} = 1 + \frac{2}{R}(r-R) + \frac{1}{R^2}(r-R)^2, \quad (3)$$

one can rewrite the remaining surface-related integral and transform the energy expression as follows:

$$E = b_{\rm vol} A \quad (4a)$$

$$+ \int_\Sigma R^2 d\Omega \int_0^\infty (\eta - b_{\rm vol}\rho) dr \quad (4b)$$

$$+ \int_\Sigma 2R d\Omega \int_0^\infty (\eta - b_{\rm vol}\rho)(r-R) dr \quad (4c)$$

$$+ \int_\Sigma d\Omega \int_0^\infty (\eta - b_{\rm vol}\rho)(r-R)^2 dr. \quad (4d)$$

Above, expressions (4b)–(4d), contain terms proportional to R^2, R^1, and R^0, respectively, thus at the same time, proportional to $A^{2/3}$, $A^{1/3}$, and A^0. In the present context, they should be interpreted as representing the surface, curvature, and Gauss-curvature contributions, correspondingly. The nuclear part of the total energy of a spherical nucleus can thus be written down as

$$E = b_{\rm vol} A + \underbrace{4\pi R^2 \mathcal{I}_0}_{b_{\rm surf} A^{2/3}} + \underbrace{8\pi R(\mathcal{I}_1 - \mathcal{I}_0 R)}_{b_{\rm cur} A^{1/3}}$$

$$\underbrace{+ 4\pi(\mathcal{I}_2 - 2R\mathcal{I}_1 + R^2\mathcal{I}_0)}_{b_{\rm curG} A^0}, \quad (5)$$

where the above mentioned correspondence relations are marked explicitly, and where

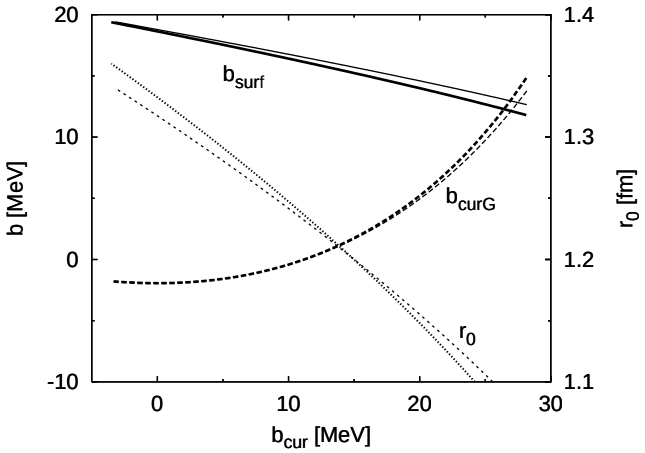

FIG. 2. Interplay between the first-order curvature ($b_{\rm cur}$, horizontal axis), the surface ($b_{\rm surf}$), and the second-order (Gauss) curvature ($b_{\rm curG}$) terms evaluated in the leptodermous expansion around $R = r_0 A^{1/3}$ of the ETF energy functional obtained with the Skyrme forces (SkM*) for ^{100}Sn (thick lines, $b_{\rm vol} = -15.387$ MeV) and ^{132}Sn (thin lines, $b_{\rm vol} = -14.289$ MeV). The corresponding values of r_0 refer to the right-hand side ordinate axis.

$$\mathcal{I}_0 = \int_0^\infty (\eta - b_{\rm vol}\rho) dr, \quad (6a)$$

$$\mathcal{I}_1 = \int_0^\infty (\eta - b_{\rm vol}\rho) r dr, \quad (6b)$$

$$\mathcal{I}_2 = \int_0^\infty (\eta - b_{\rm vol}\rho) r^2 dr \quad (6c)$$

are radial moments associated with the nuclear surface layer. Relation (5) allows to find, among others, a dependence between the curvature, surface, and Gauss-curvature terms that follow from the ETF method. To start, η and ρ [see Eq. (2)] are calculated using ETF method with Skyrme (SkM*) forces of Ref. [29], wherefrom the integrals $\mathcal{I}_0$, $\mathcal{I}_1$, and $\mathcal{I}_2$ are obtained. Next we proceed as follows: from Eq. (5), for each predefined value of $b_{\rm cur}$ we write down equality $b_{\rm cur} A^{2/3} = 8\pi R(\mathcal{I}_1 - \mathcal{I}_0 R)$ and, given $\mathcal{I}_1$ and $\mathcal{I}_0$, we deduce the implied R value. The latter quantity known was inserted into $b_{\rm surf} A^{2/3} = 4\pi R^2 \mathcal{I}_0$ and $b_{\rm curG} A^0 = 4\pi(\mathcal{I}_2 - 2R\mathcal{I}_1 + R^2\mathcal{I}_0)$ and deduce $b_{\rm surf}$ and $b_{\rm curG}$. Results of these operations are presented in Fig. 2 for ^{100}Sn (thick lines) and ^{132}Sn (thin lines) tin isotopes. It is seen from the figure that the surface energy becomes smaller when the curvature constant grows. The radius constant corresponding to the leptodermous expansion and evaluated via relation $R = r_0 A^{1/3}$ is marked on the right-hand side y axis.

Finally, let us observe the following interesting property. If we choose radius parameter R in such a way that the Gauss-curvature term [cf. the last term in Eq. (5)] is minimal i.e.,

$$R = \frac{\mathcal{I}_1}{\mathcal{I}_0}, \quad (7)$$

then the first-order curvature term [the third one in Eq. (5)] is equal to zero. Even though we are not going to impose this condition in what follows, it is instructive and helpful in analyzing the related description of the nuclear masses to know about the existence of the above correlation, especially when examining the role of the second-order (Gauss) curvature term.

The above observations confirm and illustrate the fact that the curvature terms in the nuclear energy are strictly related to the surface term as suggested in Sec. II, within a general introduction and that one cannot discuss them separately. An increase of the first-order curvature energy causes a decrease of the surface tension and vice versa. These observations will have consequences for the fitting procedures applied below.

III. FITTING THE LIQUID-DROP MODEL PARAMETERS

Our aim is to find the parameters of the liquid-drop model which correspond to the leptodermous expansion of the nuclear energy [see Eq. (1)] and the Coulomb energy of a charged nuclear drop with a diffused surface. We are going to consider separately four variants of the liquid-drop model: (a) The one of Myers and Świątecki, Ref. [24], with its original fit of parameters, referred to as MS-LD; (b) similar to the above but with the newly fitted constants, the fit using the contemporary experimental dataset and the microscopic energy corrections[4]—this variant referred to as LDM; (c) the modernized version of the liquid-drop model that contains the Gauss-curvature term, in the following referred to as ''new,'' NLD; and (d) similar to the above but containing the deformation-dependent first-order curvature term—this variant referred to as Lublin-Strasbourg version of the nuclear drop energy formula, abbreviated to LSD.

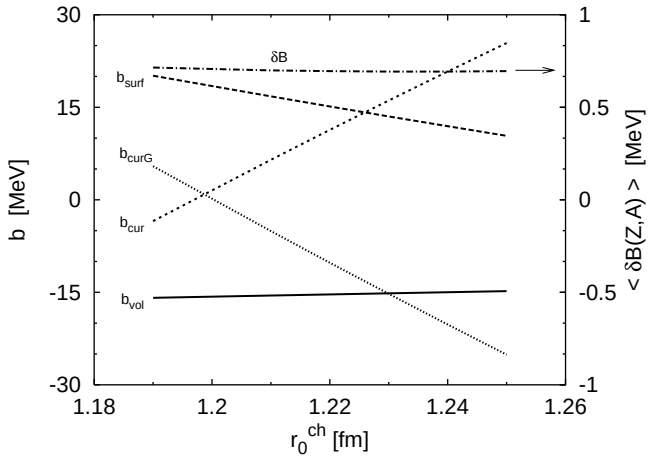

FIG. 3. Dependence of various liquid-drop model terms obtained by the least square fits to the experimental masses as functions of the Coulomb radius constant r_0^{ch}. The corresponding rms deviation of the differences between the theoretical and experimental binding energies $\langle \delta B \rangle$ refers to the right-hand side ordinate axis.

We begin by presenting the main features of the liquid-drop energy dependence on the surface-curvature terms.

A. Liquid-drop masses with curvature terms: Characteristic features

We assume, in accordance with the usual rules of the liquid-drop model approaches, that the mass of an atom with Z protons, Z electrons, and N neutrons is described by the following relation (cf. Refs. [18,24]):

$$M(Z,N;\mathrm{def}) = ZM_{\mathrm{H}} + NM_{\mathrm{n}} - 0.000\,014\,33Z^{2.39} + b_{\mathrm{vol}}(1-\kappa_{\mathrm{vol}}I^2)A + b_{\mathrm{surf}}(1-\kappa_{\mathrm{surf}}I^2)A^{2/3}B_{\mathrm{surf}}(\mathrm{def}) + b_{\mathrm{cur}}(1-\kappa_{\mathrm{cur}}I^2)A^{1/3}B_{\mathrm{cur}}(\mathrm{def}) + b_{\mathrm{curG}}(1-\kappa_{\mathrm{curG}}I^2)A^0 + \frac{3}{5}e^2\frac{Z^2}{r_0^{ch}A^{1/3}}B_{\mathrm{Coul}}(\mathrm{def}) - C_4\frac{Z^2}{A} + E_{\mathrm{micr}}(Z,N;\mathrm{def}) + E_{\mathrm{cong}}(Z,N), \tag{8}$$

where

$$E_{\mathrm{micr}} = E_{\mathrm{pair}} + E_{\mathrm{shell}} \tag{9}$$

is the microscopic energy containing the contributions from pairing and shell effects coming from the protons and from the neutrons. The congruence energy according to Ref. [18] is equal to

$$E_{\mathrm{cong}} = -10\ \ \mathrm{MeV}\exp(-42|I|/10). \tag{10}$$

The term proportional to $Z^{2.39}$ describes the binding energy of electrons. The surface diffuseness of the charge distribution reduces the Coulomb energy proportionally to Z^2/A.

In order to investigate the interplay between the Coulomb and nuclear energies when trying to reproduce the nuclear binding energies, we have performed a test fit to the experimental data from Ref. [20] for various choices of the charge radius constant r_0^{ch}. The results are presented in Fig. 3, where several terms of the liquid-drop model are plotted as functions of r_0^{ch}. The root-mean-square deviation of the binding energies $\langle \delta B \rangle$ is shown referring to the right-hand side vertical axis. Surprisingly, the quality of the fit depends

[4]To be able to compare our results with those of the quoted authors, the microscopic energy corrections for the lightest nuclei, more precisely, those with $Z<29$ and $N<29$, were taken from Ref. [18]; those for all heavier nuclei from Ref. [21].

only slightly on the choice of r_0^{ch} but the magnitudes of the first- and of the second-order curvature terms change dramatically with r_0^{ch}. It is seen that for $r_0^{ch} \approx 1.2$ fm both curvature terms are small since they both change sign near the above r_0^{ch} value.

The results in Fig. 3 show that it is rather difficult to fix the Coulomb radius parameter from the binding energies since the corresponding dependence is a flat function. Trying to deduce the related curvature contributions when varying both curvature terms is not very easy either, since the empirical r_0^{ch} value is expected not to differ very much from the mentioned special value of about 1.2 fm for which $b_{\rm cur}$ and $b_{\rm curG}$ are small (pass both through zero). Under these conditions the fit to the fission-barrier heights could give a valuable additional criterion. In the next sections, we are going to present the results of the fit of the parameters of the traditional (i.e., without the curvature terms) liquid-drop model energy expression to the experimental masses and the liquid-drop model with the curvature terms, where the parameters are adjusted either to both the measured ground-state masses and fission-barrier heights, or to the measured ground-state masses only.

B. New parameters of the traditional Myers-Świątecki liquid-drop energy expression

Exactly the same mass expression as that of the MS-LD of Ref. [24] but with the microscopic corrections for deformation, pairing and shell effects treated as in Ref. [21] and the new estimate of the congruence energy ($E_{\rm cong}$, Ref. [18]) was used to obtain the best fit to the 2766 empirical binding energies from Ref. [20] of the isotopes with the proton and neutrons numbers larger or equal to eight. Following a practical recipe used in Ref. [18], when adjusting the parameters of the macroscopic model energy expression

$$\begin{aligned} M(Z,N;\mathrm{def}) = {} & ZM_{\rm H} + NM_{\rm n} - 0.000\,014\,33Z^{2.39} \\ & + b_{\rm vol}(1-\kappa_{\rm vol} I^2)A + b_{\rm surf}(1-\kappa_{\rm surf} I^2)A^{2/3} \\ & + \frac{3}{5}\frac{e^2Z^2}{r_0^{ch}A^{1/3}} - C_4\frac{Z^2}{A} + E_{\rm def}(Z,N) \\ & + E_{\rm pair}(Z,N) + E_{\rm shell}(Z,N) + E_{\rm cong}(Z,N), \end{aligned} \tag{11}$$

we take into account the nuclear deformations. In particular, the macroscopic part of the total energy $E_{\rm def}$ is taken from tables of Ref. [21] ($E_{\rm def}$ is defined as the difference between the macroscopic energy of a nucleus at the equilibrium deformation and the energy of the same but spherical nucleus, plus the sum of the shell and pairing energies taken at the actual equilibrium deformation). The same approximation is used when fitting the parameter sets of other variants of the model presented in this paper.

The new set of parameters obtained by fitting the nuclear masses (but not using any information about the fission barriers, similarly as in Ref. [24]), is given below. For comparison, the old values of the parameters taken from the above reference are given in parentheses,

$$b_{\rm vol} = -15.8484 \ \ (-15.667) \ \ \mathrm{MeV}, \tag{12a}$$

$$b_{\rm surf} = 19.3859 \ \ (18.56) \ \ \mathrm{MeV}, \tag{12b}$$

$$\kappa_{\rm vol} = 1.8475 \ \ (1.79), \tag{12c}$$

$$\kappa_{\rm surf} = 1.9830 \ \ (1.79), \tag{12d}$$

$$r_0^{ch} = 1.18995 \ \ (1.2049) \ \ \mathrm{fm}, \tag{12e}$$

$$C_4 = 1.19949 \ \ (1.21129) \ \ \mathrm{MeV}. \tag{12f}$$

The rms mass deviation corresponding to the new set of parameters and the microscopic corrections from Ref. [21] is $\langle \delta M \rangle = 0.732$ MeV; an analogous quantity for the old set of the liquid-drop parameters and the same microscopic corrections is $\langle \delta M \rangle = 4.477$ MeV. The rms mass deviation obtained with the new parameter set is comparable with that of the Thomas-Fermi model ($\langle \delta M \rangle = 0.757$ MeV) and proves that the liquid-drop approximation can reproduce the nuclear masses with a comparably high accuracy.

Let us observe that neither the old set of the liquid-drop parameters (MS-LD) nor the new one (LDM) is able to reproduce correctly the magnitudes of the experimental fission barriers. The discrepancies between theoretical and experimental fission-barrier heights of 40 nuclei that can be found in the published literature[5] are presented in Fig. 4 (for the sources, cf. Refs. [18,22,30] and references quoted there). To extract the barrier heights from the experimental, we have used a similar prescription as that in Ref. [22], namely, we define the barrier height V_B as a difference between the liquid-drop saddle-point energy and the ground-state energy deduced from the ground-state masses. It is seen in Fig. 4 that the traditional MS-LD model overestimates the barrier heights of the lighter nuclei by about 10 MeV and by about 3–4 MeV those of the heavier ones. Our new fit of parameters of this traditional LDM overestimates the barrier heights even more significantly (Fig. 4). Does it mean that the liquid-drop model is unable to reproduce with a more respectable accuracy the positions of the fission saddle-point energies? In order to answer this question, we have performed additional tests in which we have made either a simultaneous fit of the liquid-drop model parameters to the

[5] In this paper, we use only those experimental barrier heights that can be found in the published sources; they correspond to 40 nuclei with $75 \leqslant A \leqslant 252$. This information concerns four relatively light nuclei, viz., $^{75}_{35}$Br and $^{90,94,98}_{40}$Mo and the whole rest of nuclei clearly separated in terms of Z ($Z > 70$). The barriers of these four lightest nuclei present the same type of difficulties for all the variants of the model, including that introduced in this paper (LSD). As far as the barriers of $Z > 70$ nuclei are concerned, some variants of the model describe them very well, some variants are clearly less satisfactory (for details see below).

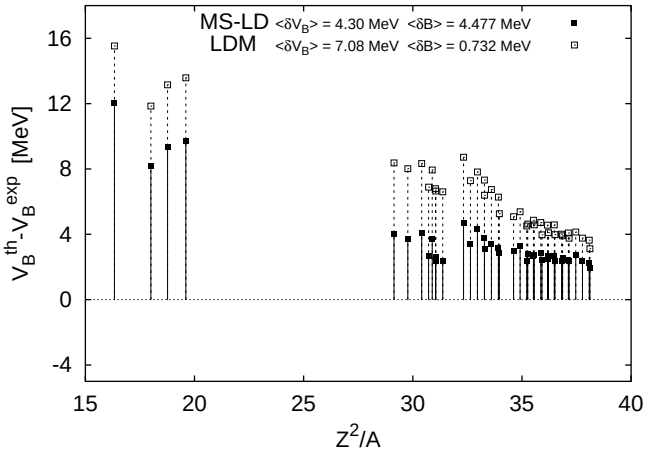

FIG. 4. The differences between the theoretical and experimental fission-barriers heights obtained with the traditional MS-LD [24], solid symbols, and its modern version LDM, open symbols, obtained by the new fit to the presently known masses, and microscopic corrections from Ref. [21]. No information on the barrier heights has been used in the fitting procedure in this case.

experimental masses and fission-barrier heights, or the fits limited to the nuclear masses. The results are presented in the next sections.

C. Liquid-drop model with curvature terms

The purpose of the following discussion is to examine the influence of the two curvature terms introduced earlier through relations (1) and (8). We would like to adjust the parameters of the curvature-extended liquid-drop model both to the huge body of the experimental nuclear binding energies known today and, if necessary, to the experimental fission-barrier heights. The nuclear mass expression of Eq. (8), compared to that by Myers and Świątecki in Eq. (11), contains the curvature terms of the first and of the second orders. The fit to the experimental masses and fission-barrier heights will be performed in three different ways: the one where only the second-order curvature term was included, another one with the first- and the second-order curvature terms, and finally, the one with the first-order curvature term only. In particular, it will be shown that taking into account the Gauss-curvature (second-order) term, which is A and deformation independent but may possibly introduce a strong dependence on the isospin factor $I=(N-Z)/(N+Z)$, improves the quality of the mass fit provided the surface tension and related coefficients were fitted to the fission barriers. It influences indirectly the fission-barrier heights through an extra (Z,N) dependence in all other simultaneously fitted parameters.

We proceed to discuss the results of the three variants of the fitting procedure separately.

1. Gauss-curvature term

In order to study the effect of the Gauss-curvature term alone on the liquid-drop energy expression we set the first-order curvature term to zero, $b_{\rm cur}=0$, thus assuming for the moment that the barrier heights can be described by the competition between the surface and Coulomb contributions only, very much like in the traditional liquid-drop model approaches. When discussing the particular case of spherical nuclei (but the conclusions drawn apply to some extent to the moderately deformed nuclei as well), it was shown, cf. Eqs. (4)–(6), that if one sets $b_{\rm cur}=0$ then necessarily $b_{\rm curG}\neq 0$.

TABLE I. The parameters of the liquid-drop model fitted to the measured atomic masses only (LDM and LSD) and to experimental barriers heights and masses (NLD).

Term	Units	LDM	NLD	LSD
$b_{\rm vol}$	MeV	−15.8484	−15.4721	−15.4920
$\kappa_{\rm vol}$		1.8475	1.6411	1.8601
$b_{\rm surf}$	MeV	19.3859	17.0603	16.9707
$\kappa_{\rm surf}$		1.9830	0.7546	2.2938
$b_{\rm cur}$	MeV			3.8602
$\kappa_{\rm cur}$				−2.3764
$b_{\rm curG}$	MeV		10.3574	
$\kappa_{\rm curG}$			13.4235	
r_0	fm	1.18995	1.21610	1.21725
C_4	MeV	1.1995	0.7952	0.9181
$\langle\delta B\rangle$	MeV	0.732	0.814	0.698
$\langle\delta V_B\rangle$	MeV	7.08	1.90	3.56
$\langle\delta V_B\rangle(Z>70)$	MeV	5.58	1.56	0.88

To fit the parameters of the model in this case, we use the fact that only some of them influence the fission barriers and we proceed as follows. First, for each value of the charge radius (r_0^{ch}), we fix the surface coefficients $b_{\rm surf}$ and $\kappa_{\rm surf}$, by making the least square fit to all experimental fission-barrier heights listed in Ref. [18]. Then the charge radius and all other than the surface-tension LDM parameters in Eq. (8), including the Gauss-curvature term, are adjusted by the least square fit to the experimental binding energies of 2766 isotopes with $Z,N\geqslant 8$ taken from Ref. [20].

The parameters of such an NLD formula are listed in Table I. The mean-square deviation of the theoretical and experimental binding energies $\langle\delta B\rangle=0.814$ MeV is only slightly larger than that of $\langle\delta B\rangle=0.732$ MeV, obtained with the refitted parameters of the traditional LDM model as described in Sec. III B. However, the fission-barrier heights are now much better reproduced. The rms deviation of the barrier heights for all treated nuclei is $\langle\delta V_B\rangle=1.90$ MeV, while for the LDM we found $\langle\delta V_B\rangle=7.08$ MeV (see in Fig. 4). Including the isospin-dependent Gauss-curvature term improves the agreement with the experimental barrier heights, nevertheless the corresponding new set of parameters does not reproduce perfectly the barriers. It is seen in Fig. 5, open symbols, that the barriers of the light isotopes ($A<100$) are overestimated by about 4 MeV and the barriers of nuclei with $A\sim 180$ are underestimated by about 3 MeV, while the barrier heights of the heaviest nuclei are overestimated by, on the average, 1.5 MeV. Thus our procedure provides, on the average, an improved fit to the experimental fission-barrier heights, but it does not reproduce very well neither Z^2/A nor A dependence of them.

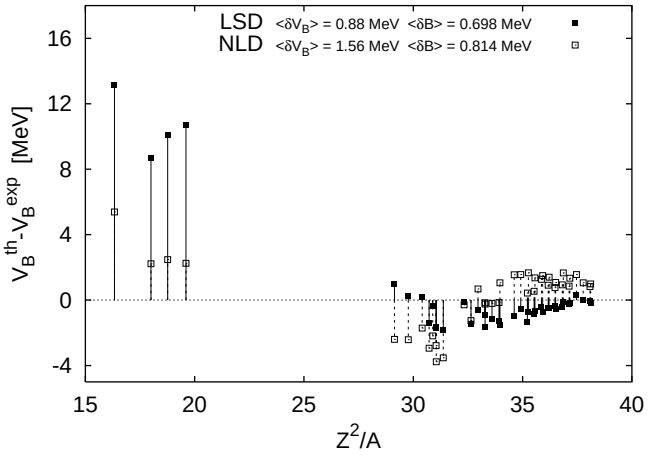

FIG. 5. Differences between the theoretical and experimental fission-barrier heights obtained with an NLD model containing no first-order curvature term (open symbols) and with the LSD model that contains the first-order curvature term (solid symbols). The LSD parameters were adjusted to the experimental binding energies only, while the NLD ones were fitted to the measured fission-barrier heights and to the masses. The rms deviation for the LSD barriers is 3.56 MeV, but reduces to 0.88 MeV when the lightest four nuclei are disregarded. (For these four nuclei the congruence effects, that are not a part of the traditional liquid-drop model considerations, are most likely important.)

Below we show that a possible remedy is to include the first-order curvature term.

2. Both curvature terms

It is known that the light nuclei have saddle points at very elongated shapes, whereas the saddle points in the actinide and *trans*-actinide nuclei correspond to rather compact shapes. The surface and curvature terms depend on deformation in a very similar way for small and even moderate deformations [31], while at large deformations the differences become pronounced. This feature will be used to improve the description of the barriers.

Performing the least square fit to the experimental fission-barrier heights for a fixed charge radius (r_0^{ch}) we have obtained the surface, $b_{\rm surf}$ and $\kappa_{\rm surf}$, and the curvature, $b_{\rm cur}$ and $\kappa_{\rm cur}$ coefficients, all other parameters being insensitive to the barriers. The charge radius constant as well as the rest of the parameters of the deformation independent terms in Eq. (8) were obtained as before by the least square fit to the known experimental masses of Ref. [20]. The rms deviation from the experimental data obtained with such a procedure is 0.844 MeV for 2766 masses and only 1.06 MeV for the fission barriers. The parameters obtained through this procedure give a very strong dependence of both curvature terms on the reduced isospin, i.e., the corresponding κ coefficients are large. We find $b_{\rm cur}=-8.219$ MeV, $\kappa_{\rm cur}=38.92$, and $b_{\rm curG}=21.82$ MeV, $\kappa_{\rm curG}=25.0$. This dependence leads to the negative first-order curvature contribution for the light nuclei ($A<130$) [recall that the corresponding contribution is $b_{\rm cur}(1-\kappa_{\rm cur}I^2)$, and thus for I^2 small, the total contribution of this term is negative].

The next attempt, according to the procedure that employs both curvature terms was to fit all ten parameters of the model, Eq. (8), to the experimental binding energies *only*. This lead to the rms deviation from the experimental masses equal to 0.693 MeV, but the fission barriers obtained in this way were up to 20 MeV, too high for the light nuclei with $A<100$, while for the heaviest nuclei they were by about 2 MeV, too small. These unsatisfactory results lead us to examine more thoroughly the use of the first-order curvature term only i.e., by setting by definition the Gauss-curvature term to zero, as discussed in the following section.

3. First-order curvature term and the LSD parameter set

It turns out that the liquid-drop model, which in addition to the volume, surface, and Coulomb terms contains only the first-order curvature term gives the most satisfactory results, as presented below. The parameters of this LSD variant of the macroscopic model are fitted to the nuclear masses and *not* to the fission barriers. The LSD parameters obtained by fitting to the 2766 experimental masses of Ref. [20] are listed in Table I. The differences between the theoretical and experimental barrier heights are presented in Fig. 5, full symbols. Now the mean-square deviation of the binding energies amounts to $\langle \delta B\rangle=0.698$ MeV, while the mean-square deviation of the barrier heights $\langle \delta V_B\rangle=3.56$ MeV; but it decreases to only 0.88 MeV when the four lightest nuclei are disregarded i.e., when only the nuclei with $Z>70$ are considered.

As it is seen the parametrization of the barrier heights for heavier nuclei with $Z>70$ is improved considerably. The fission barriers obtained with the LSD model are closer to the experimental ones as compared to analogous results obtained in Ref. [18] with the Thomas-Fermi model (MS-TF); this is illustrated in Fig. 6, top. The difference between the MS-TF and the measured barriers are plotted in the bottom part of Fig. 6. It is seen that for heavier nuclei the agreement between the experimental data and the LSD fission barriers (Fig. 5) is even better than that for the MS-TF model, while for the light isotopes ($A<100$) both models give comparable fission barriers, but higher than the experimental ones by ≈ 10 MeV. This large discrepancy between the theoretically predicted fission-barrier heights and the measured values for light nuclei could originate from the fact that their fission barriers are very broad and the saddle points are very close to the scission points. At such configurations it could happen that the negative congruence energy (nearly) doubles, as suggested in Ref. [18], and as a consequence the fission-barrier heights calculated within such an approach could get much closer the experimental ones. Here we do not examine this type of effects because the microscopic origin of the congruence effects exceeds the framework of the classical model.

The role of the curvature term together with its dependence on isospin needs to be still analyzed in more detail. We shall examine the above questions in the following section.

The calculated LSD masses of 2766 nuclei are compared with the measured ones in Fig. 7. The lines join the points corresponding to the common-isotope chains. A part of the observed local discrepancies may originate from the microscopic corrections to the macroscopic energies that were

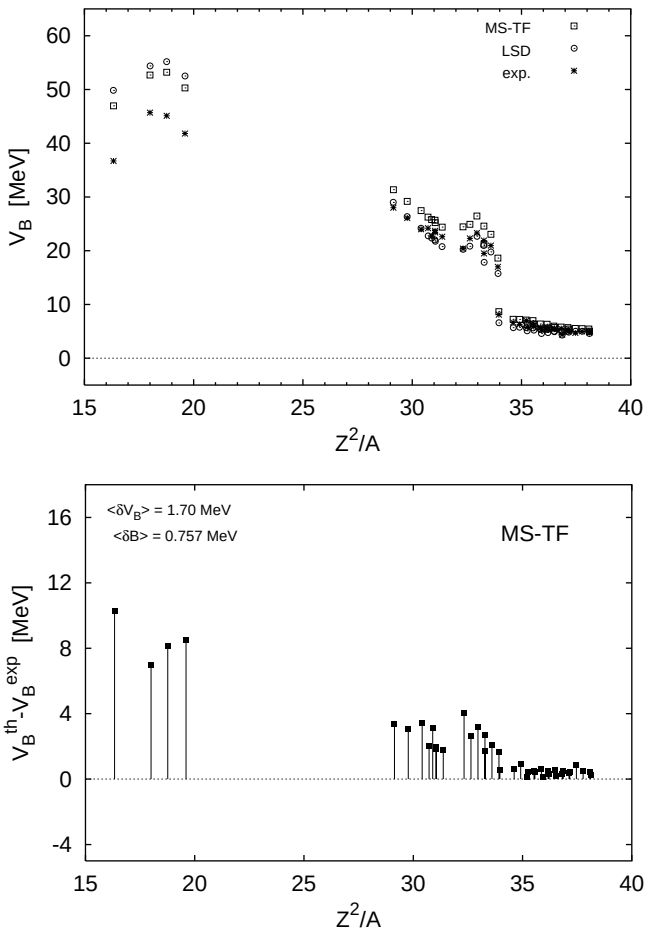

FIG. 6. Experimental fission-barrier heights (see Refs. [18,22,30] and references cited therein), asterisks, compared to the theoretical ones obtained with the LSD (circles), and the Thomas-Fermi models of Ref. [18], open squares, (top). The differences between the Thomas-Fermi and experimental fission-barrier heights are plotted in the bottom diagram.

evaluated in Ref. [21], assuming the same deformations for the proton and neutron distributions. The self-consistent calculations made in Refs. [32,33] show that in the ground state, the proton and the neutron distributions are not equally deformed. A rough estimate made in Ref. [34] within the Hartree-Fock-Bogoliubov approximation with the Gogny force shows that this effect can change the ground-state energy by $\approx \pm 0.5$ MeV. The effect of deformations that are different for the proton and neutron distributions can be incorporated to the macroscopic-microscopic models by introducing an additional term; this aspect is not going to be developed in the present paper. The form and magnitude of the term responsible for the change of the macroscopic energy due to the deformation difference of both kinds of particles was estimated in Ref. [35] within the extended Thomas-Fermi model with the Skyrme forces.

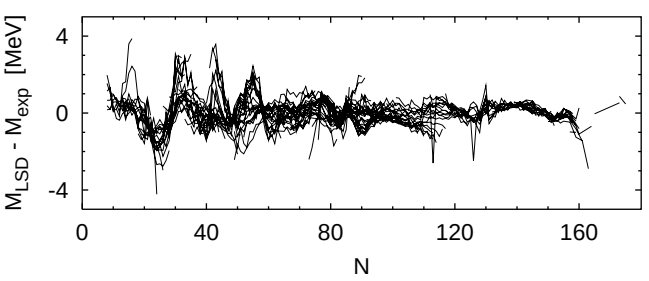

FIG. 7. Difference between calculated (LSD) and measured (expt.) masses for 2766 nuclei from the tables of Antony [20]. Lines connect the isotopes of each given element.

TABLE II. Root-mean-square deviations (in MeV) of the theoretical and the experimental binding energies of isotopes with Z and N greater or equal to 8. The experimental masses are taken from the Audi-Wapstra tables (1654 isotopes) and from Antony [20] compilation (2766 isotopes). In the first column, the numbers of experimental masses are indicated as used when fitting the parameters for the LSD variant of the present article as well as for the Thomas-Fermi and Hartree-Fock with Skyrme parameter set MSk7. The second and third columns contain the performance test and the ''extrapolation test'' for the fits with the numbers of masses given in the head of those columns.

Model	rms (2766)	rms (1654)
LSD(2766)	0.698	0.610
LSD(1654)	0.711	0.600
TF-MS(1654)	0.757	0.655
MSk7(1888)	0.828	0.738

To estimate the ''performance stability'' of a given parameter fit it is instructive to examine, among others, how a given mass formula fitted to a certain ''narrow'' mass range performs in an extended mass range and vice versa. For instance, with the LSD parameter set fitted to 1654 isotopes from the Audi-Wapstra tables we may predict the 2776 masses corresponding to the compilation of Antony [20] and by taking the corresponding differences we may calculate the implied rms deviations that illustrates the ''predictive power'' of the model and its parametrization. Such a comparison is presented in Table II for the LSD parameter set as well as for two other models indicated. For comparison, also an inverse test has been examined i.e., estimating the performance quality when going from a broader mass range to a narrower one. Results in Table II indicate among others a remarkable stability or ''predictive power'' of the LSD approach. By fitting the parameters to the 1654 masses and predicting the result for the 2776 masses, we obtain the rms deviation of 0.711 MeV, i.e., only 13 keV worse than the direct fit to the 2776 masses, the latter giving the rms of 0.698 MeV.

IV. FISSION BARRIERS AND PROPERTIES OF THE POTENTIAL ENERGY SURFACES AROUND THE SADDLE POINTS

It is interesting to compare the fission-barrier profiles obtained with different parameter sets of the liquid-drop model. In Fig. 8 the fission barriers obtained with the traditional Myers-Swiątecki (MS-LD), with the new Gauss-curvature dependent (NLD), and that with the first-order curvature

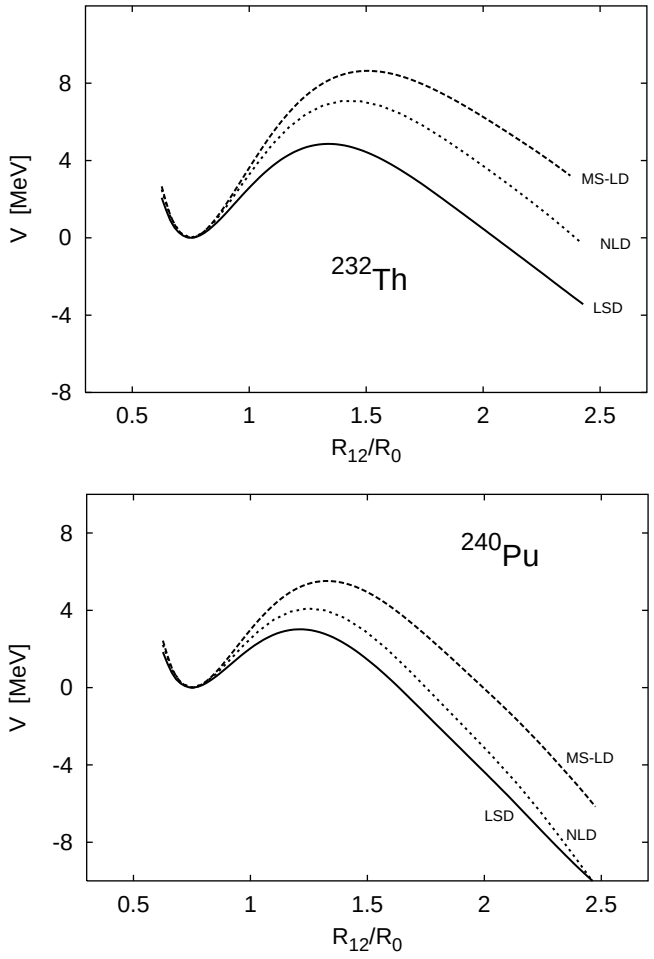

FIG. 8. Liquid-drop fission barriers for ^{232}Th (top) and ^{240}Pu (bottom) obtained with the LSD, NLD, and MS-LD sets of parameters.

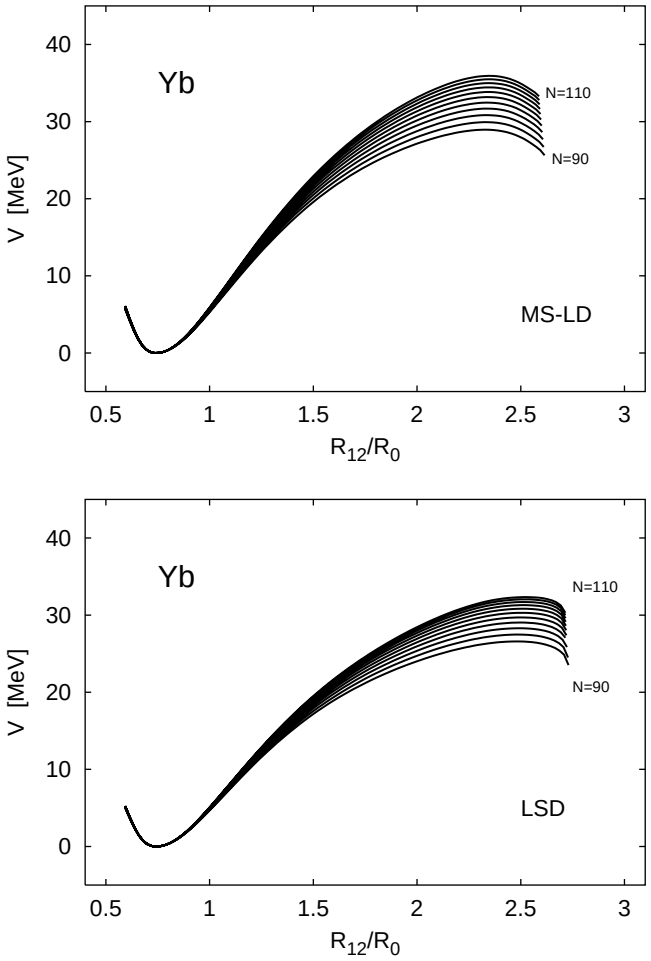

FIG. 9. Liquid-drop fission barriers for Ytterbium nuclei according to the traditional (MS-LD) approach (top) and the curvature dependent formulation of the liquid-drop model with the LSD parametrization (bottom). According to earlier predictions the Ytterbium range nuclei are likely to be sufficiently stable at the high spins to form the hyperdeformed configurations and the corresponding rotational bands.

term (LSD) liquid-drop models are plotted for ^{232}Th (top) and ^{240}Pu (bottom). It is seen that in spite of the differences in the barrier heights the slopes from the saddle to scission points are similar in all three approaches. The barriers are plotted as functions of distance R_{12} (in R_0 units) between the fission fragments. Each barrier point was minimized with respect to all even β_λ deformations with $\lambda \leqslant 14$.

The neutron number dependence of the fission barriers of Yb isotopes evaluated with the MS-LD and LSD parameter sets are presented in Fig. 9. This nuclear range is of particular interest for the hyperdeformation studies and several, so far unsuccessful experimental tests have been already attempted. Each curve is drawn up to the deformation point close to the scission point. It is seen that the LSD barrier heights are a few MeV smaller than those of MS-LD model and that they grow slower with neutron number. Also, the MS-LD barriers are ''shorter'' than the LSD ones. The fission-barrier profiles and their correct description together with the saddle-to-scission path length are important when studying the properties of, for e.g., super or hyperdeformed nuclei. In this paper, we are not going to go into more details leaving the corresponding discussion to a forthcoming paper.

Instead, we would like to examine and illustrate on some examples the stiffness of the potential energy surface with respect to higher-multipolarity deformations for the elongations that are close to the saddle and/or scission configurations.

This latter aspect is very important in the studies of, for e.g., multipath fission mechanisms, where the shell energies corresponding to the relatively exotic (e.g., high-multipolarity) deformations may provide competitive fission mechanisms. Such a problem arises also at high spins and therefore will also become important for the new generation of the calculations aiming at the hyperdeformation effect. In Fig. 10, the cross sections of the potential energy surfaces obtained with the MS-LD and LSD approaches on one hand, and with the Yukawa-Folded energy expression with parameters from [36] on the other hand, are plotted for ^{172}Yb at $\beta = 2$ as functions of β_4 (top), β_6 (middle), and β_8 (bottom). It is seen that the stiffness properties with respect to these deformations are almost the same in the case of the first two

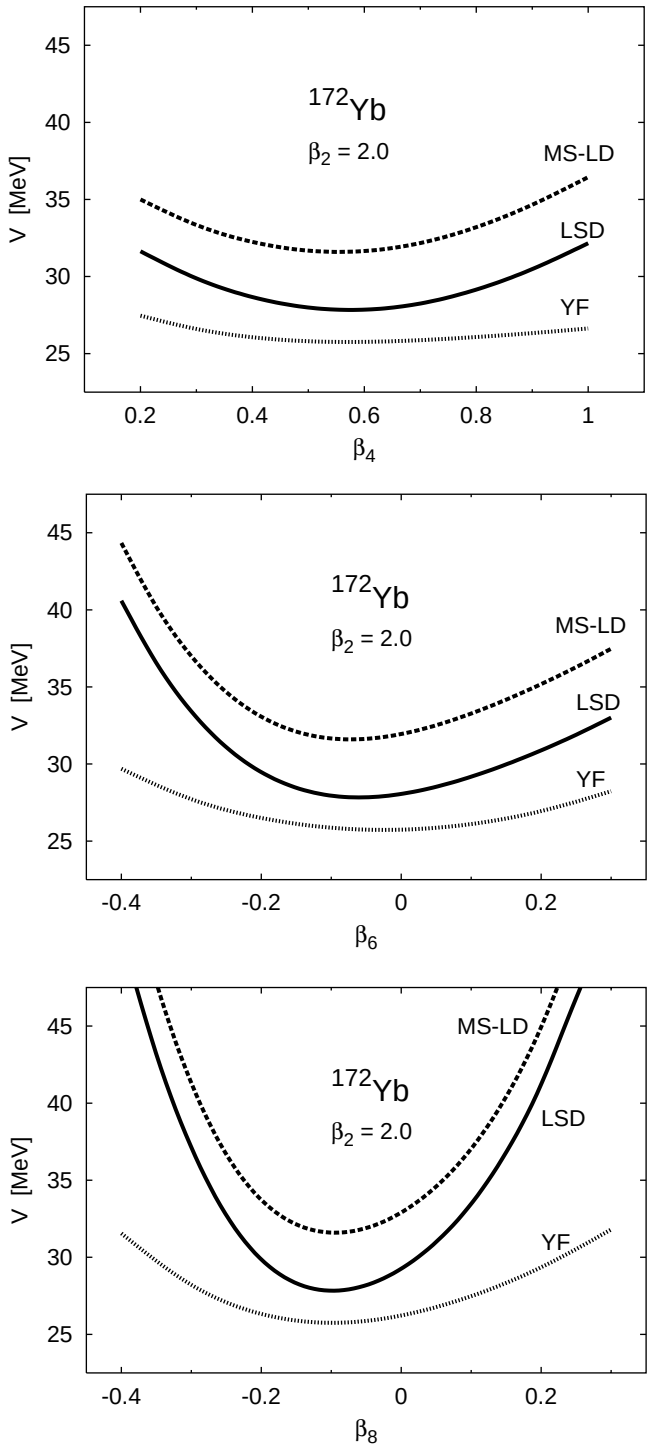

FIG. 10. Traditional (MS-LD) and curvature dependent (LSD) liquid-drop energy of ^{172}Yb around the saddle point ($\beta_2=2.0$, $\beta_4=0.582$, $\beta_6=-0.058$, $\beta_8=-0.108$, $\beta_{10}=-0.001$, $\beta_{12}=0.020$) as a function of the deformation β_4 (top), β_6 (middle), and β_8 (bottom). For comparison the Yukawa-Folded (YF) macroscopic model results are shown.

compared models. The YF approach cannot distinguish in any significant manner between, say, $\beta_4=0.5$ and $\beta_4=1.0$ (the corresponding energy difference is smaller than 1 MeV compared to about 5 MeV in the case of the other two approaches) and varies only weakly in terms of the higher-order multipoles. This very strong indifference of the YF approach with respect to significant variations of the nuclear surface at strong elongation was considered for some time already as a weakness of the latter approach, cf. Ref. [37].

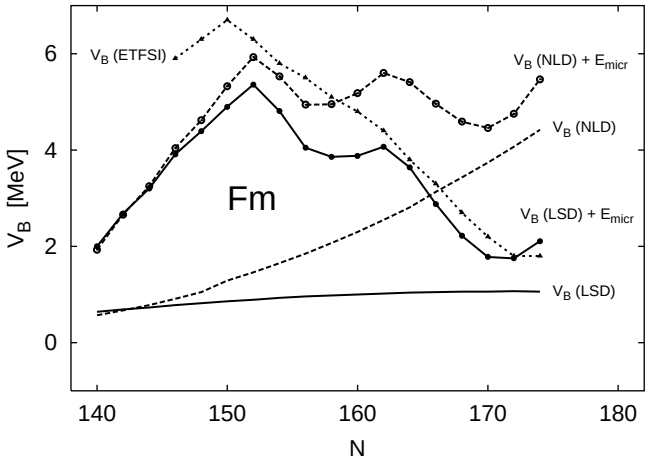

FIG. 11. Fission-barrier heights V_B of Fermium isotopes evaluated as the difference between the liquid-drop saddle-point energy and the ground-state energy containing the microscopic corrections. The solid lines with the full dots correspond to the barriers calculated with the curvature dependent (LSD) model, while the dashed lines with open circles represent the barriers calculated with the liquid-drop model without curvature term (NLD). The difference between the full and the dotted lines is equal to the ground-state microscopic correction taken from the tables [21]. The fission barriers obtained within the extended Thomas-Fermi model with the Skyrme interaction (ETFSI) [38] are drawn for comparison.

In Fig. 11 the fission-barrier heights of several Fm isotopes calculated with the LSD and NLD sets of parameters are compared with the fission-barrier heights obtained in Ref. [23] within the extended Thomas-Fermi model with the Skyrme interaction (ETFSI). It is seen that the barrier heights obtained with the NLD and LSD parameters are close to each other for the light Fm isotopes, while for the heaviest ones one may notice a significant (3 MeV) difference between the two families of the barrier heights. This decrease of the barrier heights with increasing neutron number N obtained in the LSD model for heavy Fm isotopes is confirmed by the ETFSI results [23].

The logarithms of the experimental lifetimes, T_{sf}, are plotted for comparison, in Fig. 12. It is known from the macroscopic-microscopic type of calculations that it was almost impossible to reproduce the spontaneous fission lifetime T_{sf} systematics for the chain of Fm isotopes. For the majority of the theoretical calculations, the spontaneous fission lifetimes of heavier Fm isotopes are too long, while for the light and medium-heavy isotopes they are relatively well reproduced. An attempt in Ref. [39], within the macroscopic model that contained no curvature terms confirmed the existence of the same deficiency. Such a discrepancy in the systematics originates probably from too strong N dependence of the macroscopic fission-barrier heights; a new parametrization can be seen as a step into a right direction.

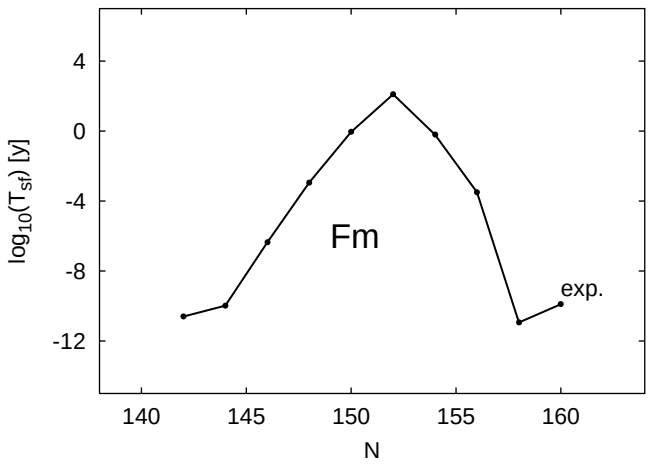

FIG. 12. Logarithm of the spontaneous fission lifetime [in years] of Fm isotopes. The full dots represent the experimental values. (cf. theoretical estimates in Fig. 11).

V. SUMMARY

We have shown that it is possible to reproduce simultaneously and with a reasonable precision the ground-state binding energies and fission-barrier heights of nuclei within the liquid-drop model containing the first- and/or the second-order curvature terms. Out of three variants of the model discussed in detail in this paper, the one abbreviated LSD (Lublin-Strasbourg drop) offers the highest precision in the description of masses and fission barriers; it also has a remarkable stability property with respect to extrapolation from narrower to the broader range of nuclei.

The traditional (i.e., without the curvature terms) liquid-drop model energy expression, abbreviated LDM, with the parameters adjusted to the experimental masses only, reproduces remarkably well the experimental masses but gives the barrier heights about 3–15 MeV larger than their measured values.

The liquid-drop model with parameters fitted simultaneously to the experimental binding energies and barrier heights can reproduce rather well both types of data when it contains the A independent but isospin-dependent second-order curvature (Gauss) term. This almost traditional expression, i.e., without the first-order curvature term, but with the surface tension adjusted to the experimental barrier heights, abbreviated NLD, reproduces on the average the right positions of the saddle points; but gives a rather poor systematic dependence of the barrier heights on Z^2/A.

The LSD variant of the liquid-drop model contains the term proportional to $A^{1/3}$ (first-order curvature term) and no Gauss-curvature term. It can reproduce the experimental binding energies and the fission-barrier heights with an accuracy comparable to or better than the Thomas-Fermi model of Ref. [18], or the HF+BCS model with Skyrme forces of Ref. [23]. Perhaps surprisingly, its parameters are adjusted to the experimental binding energies only—no information about the fission barriers has been used to fit the LSD variant parameters. Yet, it gives a correct description of the masses and the fission barriers, with the performance comparable to or better than that of other models. It gives simultaneously the right systematic of the barrier heights for the isotopes with $Z>70$. The most important information about these results is contained in Tables I and II of the paper.

Similarly, as in the Thomas-Fermi model of Ref. [18], the LSD fission barriers of the lighter nuclei ($A<100$) are overestimated by about 10 MeV. Here our conclusions coincide with those of Ref. [22], where the concept of the congruence mechanism has been discussed to remedy this problem. The isospin dependence of the surface and curvature terms in the LSD energy expression is qualitatively confirmed by the systematic of the spontaneous fission lifetimes of Fermium isotopes and quantitatively by the results of the ETFSI model.

In parallel with completing this study, an extension of the present considerations to the case of the nuclear rotation has been examined and a number of independent tests of performance of the LSD variant of the model through comparison to the measured barrier heights at high angular momenta has been advanced. An agreement with the results on fission barriers for a few rotating nuclei has been found comparable to that discussed in this paper for the static case [40].

ACKNOWLEDGMENTS

This work was partly supported by the Polish Committee for Scientific Research under Contract No. 2P03B 115 19 and by the Program No. 99-95 of Scientific Exchange between the IN_2P_3, France, and Polish Nuclear Research Institutions. One of the authors (K.P.) wishes to express his thanks for the warm hospitality extended to him by the Institute for Subatomic Research (IReS) and the Louis Pasteur University of Strasbourg; he is particularly indebted to the French Ministry of National Education for the invitation as P.A.S.T. guest professor that enabled the present collaboration.

[1] C.F. von Weizsäcker, Z. Phys. **96**, 431 (1935).
[2] H.A. Bethe and R.F. Bacher, Rev. Mod. Phys. **8**, 82 (1936).
[3] L. Meitner and O.R. Frisch, Nature (London) **143**, 239 (1939).
[4] N. Bohr and J.A. Wheeler, Phys. Rev. **56**, 426 (1939).
[5] D.L. Hill and J.A. Wheeler, Phys. Rev. **89**, 1102 (1953).
[6] H.v. Groote and E. Hilf, Nucl. Phys. **A129**, 513 (1969).
[7] K.A. Brueckner, J.R. Buchler, S. Jorna, and R.J. Lombard, Phys. Rev. **171**, 1188 (1969).
[8] W.D. Myers and W.J. Świątecki, Ann. Phys. (N.Y.) **55**, 395 (1969).
[9] W. Stocker, Nucl. Phys. **A215**, 591 (1973).
[10] B. Grammaticos, Z. Phys. A **312**, 99 (1983).
[11] W. Stocker, J. Bartel, J.R. Nix, and A.J. Sierk, Nucl. Phys. **A489**, 252 (1988).
[12] M. Brack, C. Guet, and H.-B. Høkansson, Phys. Rep. **123**, 276 (1984).

[13] M. Durand, P. Schuck, and X. Viñas, Z. Phys. A **346**, 87 (1993).
[14] M. Centelles and X. Viñas, Nucl. Phys. **A536**, 173 (1993).
[15] M. Centelles, X. Viñas, and P. Schuck, Phys. Rev. C **53**, 1018 (1996).
[16] D. von Eiff, W. Stocker, and M.K. Weigel, Phys. Rev. C **50**, 1436 (1994).
[17] F. Douchin, P. Haensel, and J. Meyer, Nucl. Phys. **A665**, 419 (2000).
[18] W.D. Myers and W.J. Świątecki, Nucl. Phys. **A601**, 141 (1996).
[19] G. Audi and A.H. Wapstra, Nucl. Phys. **A565**, 1 (1993).
[20] M. Antony, Nuclide Chart 2002, Impressions François, 103 Route de Marienthal, Haguenau, France; email address: ela.myelin@ires.in2p3.fr
[21] P. Möller, J.R. Nix, W.D. Myers, and W.J. Świątecki, At. Data Nucl. Data Tables **59**, 185 (1995).
[22] W.D. Myers and W.J. Świątecki, Phys. Rev. C **60**, 014606 (1999).
[23] F. Tondeur, S. Goriely, J.M. Pearson, and M. Onsi, Phys. Rev. C **62**, 024308 (2000); S. Goriely, J.M. Pearson, and F. Tondeur, At. Data Nucl. Data Tables **77**, 311 (2001).
[24] W.D. Myers and W.J. Świątecki, Ark. Fys. **36**, 343 (1967); W.D. Myers and W.J. Świątecki, Nucl. Phys. **81**, 1 (1966).
[25] H.J. Krappe, J.R. Nix, and A.J. Sierk, Phys. Rev. C **20**, 992 (1979).
[26] A.J. Sierk, Phys. Rev. C **33**, 2039 (1986).
[27] S. Trentalange, S.E. Koonin, and A.J. Sierk, Phys. Rev. C **22**, 1159 (1980).
[28] W.D. Myers and W.J. Świątecki, Ann. Phys. (N.Y.) **84**, 186 (1974).
[29] J. Bartel, P. Quentin, M. Brack, C. Guet, and H.-B. Høkansson, Nucl. Phys. **A386**, 79 (1982).
[30] K.X. Jing, L.G. Moretto, A.C. Veeck, N. Colonna, I. Lhenry, K. Tso, K. Hanold, W. Skulski, Q. Sui, and G.J. Wozniak, Nucl. Phys. **A645**, 203 (1999).
[31] R. W. Hasse and W. D. Myers, *Geometrical Relationships of Macroscopic Nuclear Physics* (Spinger-Verlag, Berlin, 1988).
[32] K. Pomorski, P. Ring, G.A. Lalazissis, A. Baran, Z. Łojewski, B. Nerlo-Pomorska, and M. Warda, Nucl. Phys. **A624**, 349 (1997).
[33] M. Warda, B. Nerlo-Pomorska, and K. Pomorski, Nucl. Phys. **A635**, 484 (1998).
[34] J.F. Berger and K. Pomorski, Phys. Rev. Lett. **85**, 30 (2000).
[35] A. Dobrowolski, K. Pomorski, and J. Bartel, Phys. Rev. C **65**, 041306(R) (2002).
[36] P. Möller and J.R. Nix, At. Data Nucl. Data Tables **26**, 165 (1981).
[37] L.-O. Jönsson, Nucl. Phys. **A608**, 1 (1996).
[38] A. Mamdouh, J.M. Pearson, M. Rayset, and F. Tondeur, Nucl. Phys. **A679**, 337 (2001).
[39] Z. Łojewski and A. Staszczak, Nucl. Phys. **A657**, 134 (1999).
[40] B. Herskind (private communication).